International Conference on Space Optics—ICSO 2012

Ajaccio, Corse

9–12 October 2012

Edited by Bruno Cugny, Errico Armandillo, and Nikos Karafolas

Dimensional stability validation and sensor calibration with sub-nanometer accuracy

Dirk Voigt

Rob H. Bergmans

International Conference on Space Optics — ICSO 2012, edited by Bruno Cugny, Errico Armandillo, Nikos Karafolas
Proc. of SPIE Vol. 10564, 105643K · © 2012 ESA and CNES · CCC code: 0277-786X/17/$18 · doi: 10.1117/12.2309057

Dimensional Stability Validation and Sensor Calibration with Sub-nanometer Accuracy

Dirk Voigt and Rob H. Bergmans
VSL Dutch Metrology Institute
Delft, The Netherlands
dvoigt@vsl.nl

Abstract—**We report on the development of measurement facilities for the calibration of ultra-precision displacement sensors and for the dimensional stability validation of materials, joint structures and sensors. A Fabry-Pérot interferometer and a double-ended heterodyne interferometer are discussed, both with a dedicated design aiming for sub-nanometer displacement measurement accuracy.**

Optical metrology; dimensional stability; sensor calibration; displacement interferometry

I. INTRODUCTION

High-end instrumentation, e.g. for space application, deals with challenging requirements on the dimensional stability of materials and assembled structures. Advanced materials and connections demand validation of medium to long-term, if not life-time, stability to the picometer level, e.g. C/SiC, CFRP and diffusion bonded junctions [1,2]. Highest level position sensing and control require displacement sensors that not only do provide picometer-level sensitivity (resolution) and precision (stability) but also accuracy. Examples are capacitive displacement sensors, offering high sensitivity and excellent linearity. These sensors demand for calibration methodologies with appropriate measurement uncertainty budgeting and traceability to international standards.

Optical displacement interferometry meets these validation and calibration needs. Non-contact optical heterodyne, homodyne and phase shifting interferometry minimize the perturbation on the sample under test and provide high sensitivity, that scales with the optical wavelength [3-6]. Versatile configurations and large displacement range are supported. Even higher sensitivity and precision for displacement measurement is supported by Fabry-Pérot interferometry (FPI), with high frequency selectivity of the optical cavity resonance [7-10]. FPI is particularly useful for the calibration of ultra-precision displacement sensors due to the versatility in the translation-actuated measurement interface, e.g. a conductive one for capacitive sensors.

Two dedicated measurement concepts are presented here: (i) a heterodyne interferometer aiming for picometer-level dimensional drift measuring uncertainty [11,12], and (ii) a FPI engineered to achieve sub-nanometer uncertainty for sensor calibration [8-10]. Highest level accuracy is facilitated by direct traceability to the VSL primary optical frequency standards.

II. DIMENSIONAL STABILITY VALIDATION

A double-ended optical heterodyne interferometer concept is employed for dimensional stability measurements [11]. The particular challenge for achieving picometer-level measurement uncertainty over longer periods of time (seconds to days) is the discrimination of intrinsic sample instability from other effects such as thermal expansion of both sample and interferometer bench. A general approach to make the setup extremely stable in its own might bear excessive costs, if feasible at all. Instead, a balanced optical configuration is chosen that minimizes the sensitivity of the instrument to such perturbations. Furthermore, an intrinsic compensation of air refractive index variations is considered by means of a refractometer in a twin interferometer configuration.

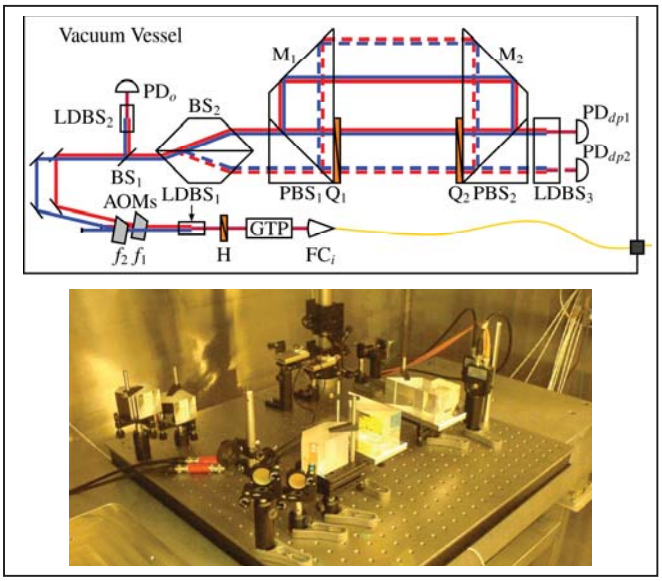

Figure 1. Stability test setup with commercial mounting components and "double-dead-path" configuration (empty interferometers). Laser source delivered through polarization maintaining fiber into pressure-sealed vessel, polarisation clean-up (GTP) and AOM heterodyne frequency splitting. Optical heterodyne reference picked up at photodetector PD_0.

Fig. 1 shows the interferometer concept as it was implemented in a first test bed [12]. The optical scheme provides a balanced configuration that is designed to minimize sensitivity to intrinsic dimensional instability of the interferometer bench. This is achieved by a common-mode rejection of perturbations acting similarly on both the sample measurement beam and the heterodyne reference beam. The scheme is double-ended such that a prismatic sample of up to 100 mm length is probed truly for intrinsic length change. A second interferometer with similar beam paths and in close proximity to the sample measurement interferometer provides refractometric functionality. A vacuum tube acts as reference path such that refractive index fluctuations of the ambient air, supposedly correlated with those in the sample section, can be corrected for. Spatial separation of the split-frequency heterodyne source beams omits periodic measurement nonlinearity, commonly originating from frequency mixing due to non-perfect polarization optical components [6]. For a more detailed description see [11,12].

Conceptually, this scheme aims for a measurement uncertainty better than 100 pm (k=2) for several hours of measurement time. The preliminary setup from Fig. 1 allowed for investigation of the intrinsic system stability. For this purpose, the differential drift signal from the two co-located interferometers was evaluated in "double-dead-path" configuration, i.e. with neither sample nor vacuum tube present. The differential twin configuration eliminates much of higher frequency noise from vibrations and thermal drift of the test rig, resulting in a differential drift reading of ±0.6 nm peak-to-peak over 23 hours, see Fig. 2(c). The comparison of pressure-shielded atmospheric air conditions with 3 mbar vacuum conditions reveals residual time-variable spatial gradients of the air refractive index in the interferometer beam paths, contributing to noise at frequencies below 0.1 Hz, see the amplitude noise spectra in Fig. 2(d). Slow drift is presumably dominated by thermal instability of the off-the-shelf mechanical mounting components, including the free-space-optics laser source delivery and optical detection.

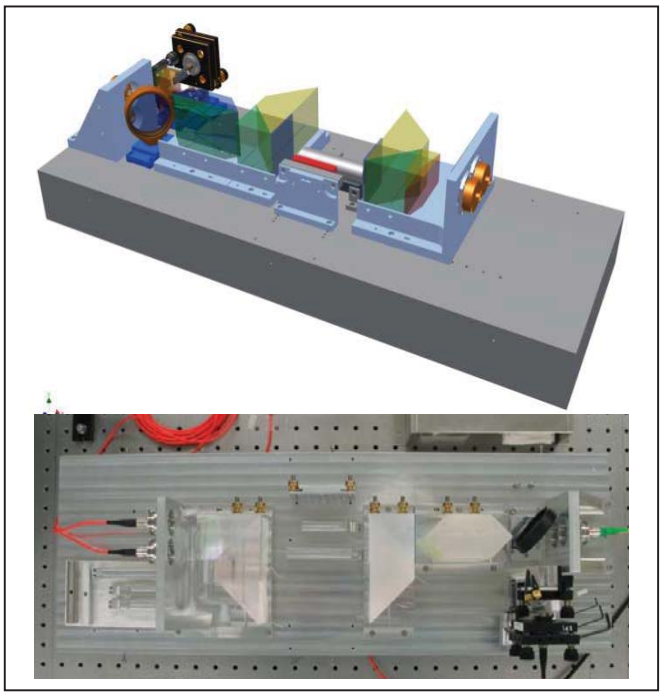

Figure 2. Custom kinematic bench with quasi-monolithic optics, fibre ports and added optical heterodyne pick-up close to the interferometer. Additional polarisers after source and before detection fibre ports are not shown, yet.

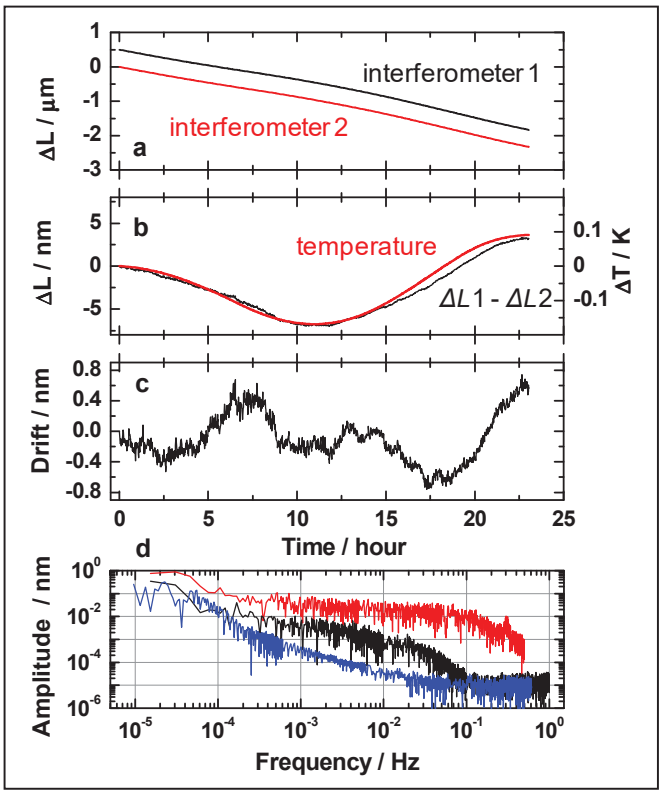

Figure 3. Double-dead-path drift in pressure-sealed shielding vessel. **(a)** Relative length changes of co-located empty interferometers: sample interferometer (red) and refractometer (black, offset by +0.5 µm for clarity). **(b)** Differential length change (black) as difference from traces in (a), and temperature change in vessel (red). **(c)** Drift estimate: length change from (b) compensated (fitted) for correlated temperature change. **(d)** Single-sided amplitude spectrum of measured intrinsic system drift: double-dead-path measurement in pressure-sealed vented vessel (black) and in evacuated vessel (blue). For comparison: 30 mm gauge block in sample interferometer (red).

In the next development phase, the custom manufactured quasi-monolithic optics components together with optical fiber coupling and a stable custom aluminum kinematic bench (optics and bench both manufactured and contributed by TNO, Delft, The Netherlands) will be employed in order to assure the balanced optical configuration, see Fig. 3. Several issues will be addressed on system component level to proceed toward picometer-level sensitivity and accuracy. Common-mode noise compensation will work only for excellent beam alignments. Hence, pointing stability will be fostered by use of polarization maintaining fibers (PMF) for source delivery and detection. Residual phase noise as from the source (AOMs, fibers) will be suppressed by pick-up of an optical heterodyne reference signal close to the balanced interferometers. Limited polarization extinction of PMF requires high quality polarization clean-up after fiber delivery to the bench in order to benefit from the spatially separated heterodyne source delivery and avoid

frequency mixing nonlinearity. Additionally, a dedicated choice of the heterodyne split frequency in the MHz range, other than previously used 10 kHz to 100 kHz, may lower residual acoustic fiber phase noise [13]. In spite of conceptual immunity against thermal expansion of the interferometer bench, any practical implementation will, supposedly, require also excellent thermal stability beyond the ±0.1 ºC stability of the VSL laboratory. Additional shielding has to provide short-term stability to the mK range. Low noise optical detection and high resolution phase measurement are mandatory (0.001º approximately corresponding to 1 pm). State-of-the-art lock-in detection instrumentation may be applicable. However, FPGA-based digital phase detection together with fast digitizers may outperform lock-in solutions in terms of sampling rate for a given phase sensitivity, digital noise filtering and high bandwidth common-mode noise suppression for sample and heterodyne reference signals [3,13]. The latter is of specific importance for the presented drift measuring interferometer. Furthermore, the refractometer functionality will be established by means of a custom vacuum cell, the implementation of which will be non-trivial due to potential ghosting beams emerging from the (AR coated) cell windows and due to alignment with any residual overall wedge of the cell.

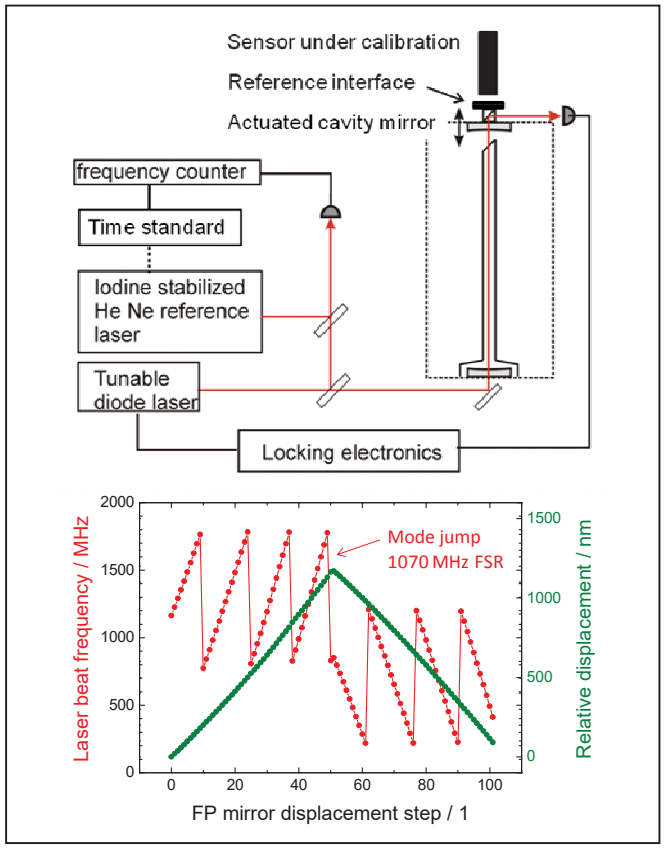

Figure 4. FPI principle and typical displacement measurement trace.

This work receives funding from the Dutch Ministry of Economic Affairs, Agriculture and Innovation, and funding within the European Metrology Research Program (EMRP). The EMRP is jointly funded by the EMRP participating countries within EURAMET and the European Union.

III. Displacement Sensor Calibration

FPI is particularly useful for characterizing stability, sensitivity, linearity and hysteresis of displacement sensors to sub-nanometer-level accuracy. The basic measurement principle is shown in Fig. 4. The upper cavity mirror is referenced to the sensor under test and actuated in order to generate high resolution displacements parallel to the vertical FP cavity optical mode axis. A tunable measurement laser is locked to the FP cavity resonance and thus follows in frequency the actuation of the mirror, i.e. any length change of the FP cavity. Direct traceability is established by recording the photo detection beat signal with a primary frequency standard, here an iodine-stabilized Helium-Neon laser. As compared with fringe-fraction measuring interferometry, periodic and interpolation errors are absent and the cavity resonance facilitates displacement resolution better than 50 pm. Additionally, climate conditions such as temperature, pressure and humidity are not only kept very stable in the VSL cleanroom laboratory but are also recorded together with the displacement readings from the sensor under test and from the locked measurement laser. This allows for the correction of air refractive index in the optical path length in the cavity. Without such correction, nanometer-level uncertainty is not achievable.

A typical measurement data trace is shown in Fig. 4. The red data points (circles) log the beat frequency of the frequency-locked measurement laser with the standard laser, while the FP mirror position is scanned with a fine stepping PZT actuator. Since the beat note detection range is limited to about 1.8 GHz with our instrumentation, the FP displacement scan range is extended by means of a repeating mode-jumping procedure. When approaching the upper beat note limit or, in the other scan direction, the zero beat note crossing, the measurement laser is unlocked, forced to a deliberate jump in frequency by ±1 FSR and relocked to the newly found cavity resonance (free spectral range here 1070 MHz, corresponding to 14 cm cavity length). The green trace shows the mirror displacement as evaluated from the beat note record together with the air refractive index correction from logged climate data.

A complex calibration measurement sequence such as shown in Fig. 4, extended displacement scan range, scan repetitions and further going drift stability investigation for a sensor under test all require an exceptional thermo-mechanical stability of the FPI. Also the axial alignment of FP cavity, actuated mirror displacement and sensor under test provide important contributions to the achievable measurement uncertainty. In order to meet these demanding requirements, a dedicated FPI design had been developed at Eindhoven Technical University [8] and studied together with NMi Van Swinden Laboratory (at that time name of VSL) [9,10].

Fig. 5 shows a cross section of the FPI and the current implementation in the VSL laboratory. The core of the design is a monolithic flexure gear used to linearly translate the upper cavity mirror with high precision. Actuation is possible in fine steps using a PZT translator and in coarse steps using a PZT-geared actuator (picomotor). The latter allows for a maximum travel of the mirror of 300 µm. Thermo-mechanical stability is established by three Zerodur spacer rods that fix the upper

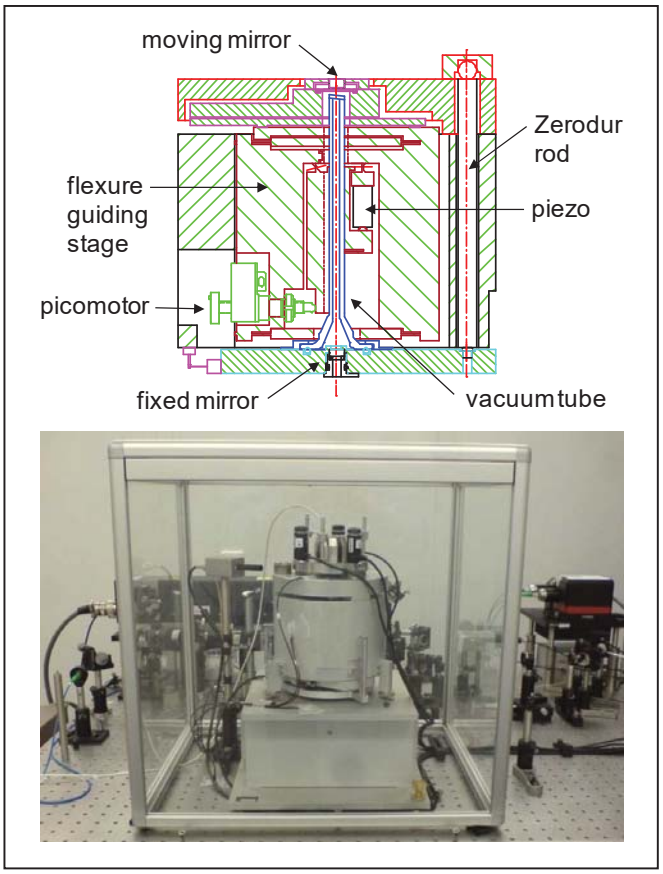

Figure 5. FPI construction and laboratory implementation.

platform disk and allow for a stable mounting of sensors under test above the actuated cavity mirror. The photograph shows a holder assembly with a capacitive sensor mounted. Sensor tilt and hold-off distance can be manipulated remotely from the neighboring viewing room using three picomotors. This facilitates sensor alignment without otherwise imposing thermal settling periods after the operator's direct manipulation at the device. Alternative to a small disk-like gauge block (not shown), other interfaces can be applied, e.g. a mirror for validation of optical interferometer displacement sensors. Likewise to Fig. 4, also a vacuum cell is shown, covering most of the volume of the optical cavity mode. To date and for practical reasons, it has not been used in evacuated mode. Air refractive index compensation as calculated for the full mode volume was sufficient for nanometer-level uncertainty. The measurement process, including fine and coarse mirror stepping and laser mode jumps, can be fully remotely controlled from the viewing room by means of a measurement software. Automization is necessary particularly for wider range scans (300 µm displacement corresponding to about 1000 FSR i.e. mode jumps).

Table 1 summarizes the uncertainty budgeting of the current VSL Metrological FPI instrumentation. Whereas the thermal stability dominates the uncertainty budget for measurements with small displacement scan range, the axial alignment of the sensor and of the FP cavity is most significant at larger range. For more details see [9].

In a recently started activity, FPI will be further developed toward displacement sensor calibration capabilities with targeted picometer-level uncertainty for the shorter displacement stroke up to 1 µm and with more flexibility in orientation other than vertical and referencing to the sensor under test. The aim will be for a more compact design, improved robustness and precision of the frequency locking of the measurement laser, including the mode jump process. Referencing the measurement laser to the VSL optical frequency comb generator can provide direct traceability to the VSL atomic clock time standard, with shorter time-averaging needs and more accuracy. This may facilitate larger measurement sampling rate and thus anticipate thermo-mechanical instability for otherwise longer lasting calibration sequences (cf. comb usage in [7,14]). Ambient climate conditions, such as humidity effects [15] or pressure fluctuations [16] limit the ultimately achievable measurement uncertainty. Recording and control of environmental parameters will be improved. For any practical calibration methodology also referencing and alignment of a sensor under test is crucial and will be investigated.

TABLE I. UNCERTAINTY BUDGET OF VSL METROLOGICAL FPI [9]

	Displacement 0.3 µm	**Displacement 300 µm**
Uncertainty contribution (standard uncertainty)	*nm*	*nm*
Frequency measurement	0.01	0.01
Laser lock	0.05	0.05
Alignment (sensor)	0.05	**10**
Cavity air gap	0.3	0.3
Brewster window	0.2	0.2
Thermo-mechanical stability	**0.5**	**0.5**
Cavity mirror tilt	0.0004	0.4
Laser gain profile	0.0002	0.002
Cavity length	0.13	0.13
Absolute air refractive index	0.00006	0.06
Total expanded uncertainty (k=2)	**1.3**	**20**
Resolution	**0.05**	**0.05**

IV. CONCLUSION

Optical displacement interferometry is a promising tool for sample stability characterization and sensor calibration to sub-nanometer-level measurement uncertainty. Two VSL development activities address these applications in the framework of current international joint research activities of EURAMET: a heterodyne interferometer for dimensional drift measurements [17] and improved instrumentation and measurement methodology of Fabry-Pérot interferometry with a focus on capacitive displacement sensor calibration [18], both targeting picometer-level measurement uncertainty. The preliminary heterodyne interferometer test setup displayed an

intrinsic stability of ±0.6 nm peak-to-peak over 23 hours and sub-30 pm noise level at a minute timescale. Considerable improvement of the system stability is expected from the implementation of the refractometric functionality by means of a vacuum reference cell and from the use of custom optical interferometer components together with a dedicated kinematic bench construction. The FPI development emerges from the current baseline of the VSL Metrological FPI, revisited in this paper. Both interferometry concepts require precise, validated mechanical alignment methodologies for interferometer and referenced sample, in addition to very stable traceably monitored ambient climate conditions.

REFERENCES

[1] J. Cordero et al., "Interferometry based high-precision dilatometry for dimensional characterization of highly stable materials", Meas. Sci. Technol., vol. 20, p. 095301, 2009.

[2] S. Ressel et al., "Ultrastable assembly and integration technology for ground- and space-based optical systems", Appl. Opt., vol. 49, pp. 4296–4303, 2010.

[3] M. Pisani et al., "Comparison of the performance of the next generation of optical interferometers", Metrologia, vol. 49, pp. 455–467, 2012.

[4] T. Schuldt et al., "Picometer and nanoradian optical heterodyne interferometry for translation and tilt metrology of the LISA gravitational reference sensor", Class. Quantum Grav., vol. 26, p. 085008, 2009.

[5] R. Schödel et al., "A new Ultra Precision Interferometer for absolute length measurements down to cryogenic temperatures", Meas. Sci. Technol., vol. 23, p. 094004, 2012.

[6] J. D. Ellis, A. J. H. Meskers, J. W. Spronck, and R. H. Munnig Schmidt, "Fiber-coupled displacement interferometry without periodic nonlinearity", Opt. Lett., vol. 36, pp. 3584–3586, 2011.

[7] M. Durand, J. Lawall, and Y. Wang, "High-accuracy Fabry-Perot displacement interferometry using fiber lasers", Meas. Sci. Technol., vol. 22, p. 094025, 2011.

[8] H. Haitjema, P. H. J. Schellekens, and S. F. C. L. Wetzels, "Calibration of displacement sensors up to 300 µm with nanometer accuracy and direct traceability to a primary standard of length", Metrologia, vol. 37, pp. 25–33, 2000.

[9] R. H. Bergmans, H. Haitjema, S. F. C. L. Wetzels, and P. H. J. Schellekens, "Calibration of nanosensors with direct traceability to the Metre", Proc. of SPIE, vol. 4401, pp. 217–226, 2001.

[10] S. J. A. G. Cosijns, Displacement laser interferometry with sub-nanometer uncertainty, PhD thesis, Eindhoven Technical University, 2004.

[11] J. D. Ellis, K.-N. Joo, J. W. Spronck, and R. H. Munnig Schmidt, "Balanced interferometric system for stability measurements", Appl. Opt., vol. 48, pp. 1733–1740, 2009.

[12] D. Voigt et al., "Toward interferometry for dimensional drift measurements with nanometer uncertainty", Meas. Sci. Technol., vol. 22, p. 094029, 2011.

[13] C. Weichert et al., "A heterodyne interferometer with periodic nonlinearities smaller than ±10 pm", Meas. Sci. Technol., vol. 23, p. 094005, 2012.

[14] J. Oulehla et al., "Evaluation of thermal expansion coefficient of Fabry-Perot cavity using an optical frequency comb", Proc. of SPIE, vol. 8082, p. 80823Q-1, 2011.

[15] P. Egan and J. A. Stone, "Absolute refractometry of dry gas to ±3 parts in 10^9", Appl. Opt., vol. 50, pp. 3076–3086, 2011.

[16] T. Q. Banh, Y. Ohkubo, Y. Murai, and M. Aketagawa, "Active suppression of air refractive index fluctuation using a Fabry–Perot cavity and a piezoelectric volume actuator", Appl. Opt., vol. 50, pp. 53–60, 2011.

[17] IND13 "Thermal design and time-dependent dimensional drift behaviour of sensors, materials and structures", JRP summary, ERMP Call 2010 Industry & Environment, www.euramet.org.

[18] SIB08 "Traceabiliy of sub-nm length measurements", JRP summary, EMRP Call 2011 SI Broader Scope, www.euramet.org.